

Study the Effect of Fluxes on Weld Penetration during Activated TIG Welding of SS304

Varun Sancheti ^{1,a}, Darsh Patel ^{1,b}, Nilesh Ghetiya ^{1,c}

Institute of Technology, Nirma University, Ahmedabad, Gujarat, India ¹

19bme144@nirmauni.ac.in ^a, 19bme083@nirmauni.ac.in ^b, nilesh.ghetiya@nirmauni.ac.in ^c

Abstract: Stainless steel is widely employed in a variety of industries, including aerospace, chemical processing, and transportation. It can be recycled indefinitely with no loss of property. The Gas Tungsten Arc Welding (GTAW) or Tungsten Inert Gas (TIG) technique is widely used for connecting thin pieces of stainless-steel. However, it is ineffective for combining heavy parts in a single pass. Activated TIG (A-TIG) dramatically enhances weld penetration up to 1.5- 4 times in a single pass. A-TIG is the centre of investigation among researchers because of its deep penetrating capacity. This article discusses the effects of particular flux powders, such as NaF and Fe₂O₃, on surface appearance and geometric shape. Weld of satisfactory appearance is produced using NaF powder as a flux in TIG welding, whereas, Fe₂O₃ powder results in a substantial increase in both the joint-penetration and weld-aspect ratio.

Keywords: A-TIG Welding (Activated Tungsten Inert Gas Welding), 17Cr–10Ni–2Mo alloy, Flux Powder, NaF (Sodium Fluoride), Fe₂O₃ (Ferric Oxide), Oxide, Penetration.

1 Introduction

Stainless steel (SS) is an alloy with excellent weldability, corrosion resistance, long service-life, formability, and non magnetic characteristics. Stainless steel is a material that is widely utilized in several industries, including automotive, rolling, chemical processing, construction, home products, and aero-space. SS can also be used at a wide variety of temperatures, from red-hot to cryogenic [1]. High-quality welds are achieved in TIG welding in almost all metals and alloys (except for alloys with a very low melting point). Although TIG welding offers several advantages, it also has some limitations. For instance, it can only weld base metals up to a certain thickness in a single pass, and there can be significant variations in weld penetration between heats. In addition, productivity gains with TIG welding tend to be relatively low [2-6]. TIG welding is often associated with low efficiency and productivity due to its slow welding speeds and the need for multiple passes to fill groove joints on thick plates or heavy-wall pipes. It may also require additional filler metals and incur extra costs for edge preparation, which can significantly increase welding time. These issues significantly reduce the appeal of TIG welding. According to [4], the activated TIG welding process offers superior penetration capability, up to 300% more than conventional TIG welding. Additionally, using an activating flux can help avoid variations in base metal compositions from one heat to another.

Although there is little information in the literature about the composition of flux powders, this knowledge is essential to determining how activated fluxes affect penetration. Activated TIG welding uses oxide powder, although there is still little information on sulphide or fluoride powder [12]. One way to improve TIG weld penetration is through the use of activated flux, which involves incorporating inorganic compounds. This method, known as activated TIG welding, has been shown to be highly effective. According to research, activated TIG welding of stainless steel can achieve a penetration depth of up to 8 mm in a single-pass weld without requiring edge preparation [7,8]. The activated flux used in this process is often applied as a suspension of powder in a solvent, allowing for a thin layer of flux to be deposited on the surface of the base metal prior to welding. Tseng et al.[11]carried out experiments and found that the activated TIG welds exhibited a narrow, deep shape with penetration depth increased by 3 times and bead width decreased simultaneously in comparison with conventional TIG welding. Kuang et al.[9] found that the penetration depth and weld aspect ratio increased in FeO and FeS as the

activating element. The TIG welds that utilized FeF₂ powder demonstrated a satisfactory surface appearance, while the welds that employed FeO and FeS produced slag and spatter. Tseng et al. [6] investigated the influence of MnO₂, TiO₂, MoO₃, SiO₂, and Al₂O₃ fluxes on weld penetration depth and weld aspect ratio in their study. Activated TIG welding was employed to enhance the joint penetration and the weld depth-to-width ratio. In this research work the influence of the Oxide Flux (Fe₂O₃) and Fluoride Flux (NaF) on weld penetration in the A-TIG welding of SS304.

2 Experimental Details

The experimental material used in this study was a commercial Fe-17%Cr-10%Ni-2%Mo austenitic 304 stainless steel alloy. *Table 2.1*, displays the chemical composition of the alloy. The dimensions of the test plates are 100 × 100 mm, with a thickness of 6 mm. The surfaces of the specimens were prepared by rough grinding with 240 grit (silicon carbide) flexible abrasive paper to eliminate impurities and cleaned with acetone prior to welding. *Table 2.2*, provides a brief of experimental parameters throughout the process, which was kept unchanged to attain uniformity in the experiment. One fluoride and one oxide compound, NaF and Fe₂O₃, were used in powdered form (*Fig. 2.3*). *Table 2.3*, displays the characteristics of the flux powder used through the experiment. To prepare for welding, the flux powder was mixed with acetone and stirred with a glass rod until it had a paint-like consistency. Then manually the resulting mixture was applied with a paintbrush to the surface of the base metal. It was applied thick enough to conceal the metal underneath, and the consistency of the flux powder coating was carefully controlled.

Table 2.1
Chemical composition (wt.%, balance Fe) of experimental alloy.

Cr	Ni	Mn	Si	N	C	P	S
17.5-19.5%	8-10.5%	2%	1%	0.11%	0.07%	0.05%	0.03%

Table 2.2
Process parameters of TIG welding experiment.

Base	Austenitic Stainless Steel SS304 (100x100x6 mm)
Weld Current	125 A
Weld Speed	150 mm/min
Electrode Gap	2 mm
Shielding Gas	99.99% Argon Gas
Gas Flow Rate	12 lit/min
Flux Powder	Ferric Oxide (Fe ₂ O ₃) & Sodium Fluoride (NaF)
Flux Solvent	Acetone

Table 2.3
Characteristic of experimental powders.

Flux powder	NaF Powder	Fe ₂ O ₃ Powder
Origin	ASES Chemical Co.	Otto Chemie Pvt ltd
Purity	99.99%	99.99%
Molar Mass	41.98816 g/mol	159.69 g/mol
Density	2.56 g/cm ³	5.24 g/cm ³
Melting Point	993 °C	1565 °C
Boiling Point	1695 °C	3414 °C
Lattice Energy	919.8 kJ/mol	14774 kJ/mol

To reduce the impact of reaction stresses, no constraints were placed on any of the test specimens during welding. The direct current electrode negative (DCEN) mode was utilized with a mechanized operating system in which the torch went at a constant speed. On the test specimens' centre line, autogenous, bead-on-plate TIG welds were applied. The electrode rod was made of tungsten and had a 2.5 mm diameter. The electrode's tip had a 45° angle and was blunt. A 99.99% pure form of argon was employed as a shielding gas. To make sure that the welding was done under the same operating

circumstances, the electrode's tip angle was grounded and the electrode gap was measured before each fresh weld.

A metal platform ([Fig 2.1\(a\)](#)) was set up to move back and forth using a motorized mechanism. It consists of worm gear underneath the platform which assists the backward and forward travelling of the same. On either end, a hook-shaped metal piece is fixed to limit the platform's mobility to a particular extent. A two-way switch ([Fig 2.1\(b\)](#)) is present to turn the motor ON/OFF and to control the direction of travel of the metal platform on which the welding workpiece is placed. A potentiometer ([Fig 2.1\(b\)](#)) was also connected in series to control the speed of the motor, hence controlling the travelling speed of the weld. It has various speed modes ranging from 30mm/min to 300 mm/min in both directions. The welding torch ([Fig 2.1\(a\)](#)) was mounted on the edge of the platform. The height of the welding torch can be adjusted by the operator and screw clamps are provided to fix the position of the torch at a certain height and angle to obtain uniform results throughout the experiment. A scale is also attached to one edge to measure the distance travelled by the platform.

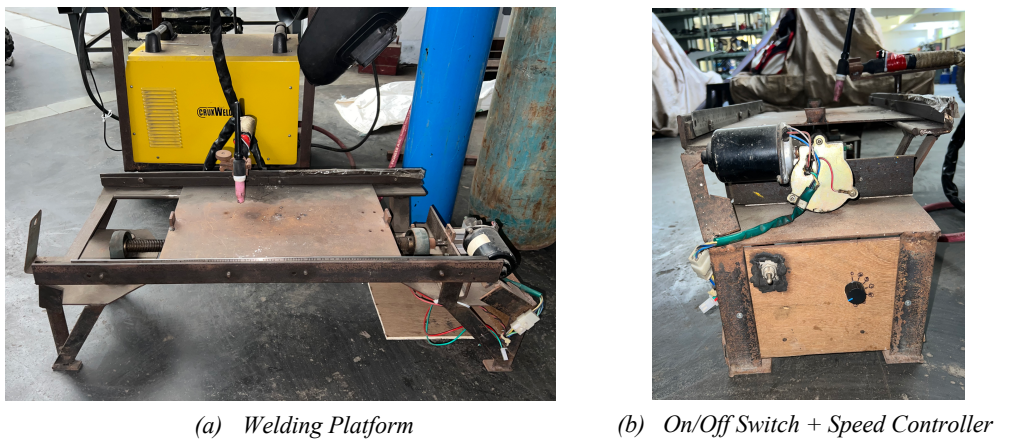


Fig 2.1. Experimental Setup for A-TIG Welding

The experiment involved applying flux powder in different patterns. We measured the differences in weld depth and penetration after applying the flux powder in different patterns. [Fig 2.2.](#) depicts the different patterns of flux paste application. [Table 2.4.](#) gives a brief description of flux paste application on the SS304 workpiece. Fig. shows the original appearance of the flux powder.

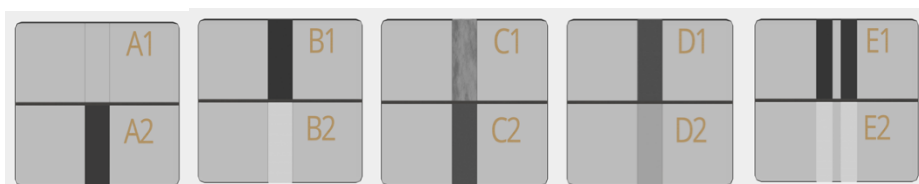


Fig 2.2. Different pattern of flux application

Table 2.4
Description of different patterns of Flux application

Sr. No.	Annotation	Pattern Description
1	A1	Without Flux Powder
2	A2	50% Oxide Flux (Fe_2O_3) + 50% Fluoride Flux (NaF)
3	B1	Only Oxide Flux (Fe_2O_3)
4	B2	Only Fluoride Flux (NaF)
5	C1	First Oxide Flux then Fluoride Flux
6	C2	First Fluoride Flux then Oxide Flux
7	D1	80% Oxide Flux (Fe_2O_3) + 20% Fluoride Flux (NaF)
8	D2	20% Oxide Flux (Fe_2O_3) + 80% Fluoride Flux (NaF)
9	E1	Oxide Flux on both sides of the welding region
10	E2	Fluoride Flux on both sides of the welding region



(a) NaF Powder



(b) Fe_2O_3 Powder

Fig 2.3. Original Appearance of Flux Powder

For different experimental conditions listed in [Table 2.4](#), different quantities of flux powder were taken by precise measurement using a digital measuring weight scale. A schematic diagram of the preparation process for the activated flux is presented in [Fig 2.4](#). After manually applying the mixture onto the specimen with a paintbrush, a layer thick enough to obstruct visual inspection of the surface below was left. Upon evaporation of the acetone, a dry powder adhered to the surface of the specimen, ready to be welded.

Once all the workpiece is dried and completely prepared, they one by one it is kept on the metal platform ([Fig 2.1\(a\)](#)) and the arc is ignited in the tungsten electrode welding torch, simultaneously the switch ([Fig 2.1\(b\)](#)) is turned to forward direction and welding is started at a constant speed. Before starting the welding, the speed of the motor is to be set at 150 mm/min as the welding speed for the experiment. The electrode gap is measured before every welding process and it is maintained at a 2 mm distance from the workpiece at all times throughout the investigation process. As a result of this process, shown in ([Fig 2.5](#)) the workpieces are uniformly welded. Then cross-section is taken of every specimen using a metal grinder machine and then grinded using a bench grinder, abrasive sheets of grits 120 – 220 – 400 – 600 – 800 to remove all the scratches and unevenness on the surface, and at last polished on the diamond polishing machine to get a mirror-like surface finish.

After welding, a USB microscope was used to take pictures of the welds' geometric form and surface appearance. Two quality criteria, namely penetration depth and bead width were used to describe the weld geometry in this experiment. To perform metallographic analysis, transverse sections were cut at multiple points along the welds. Standard procedures were followed to prepare the samples, including sectioning, mounting, grinding, and polishing until a surface finish of $0.05 \mu\text{m}$ was achieved. The samples were then etched using a solution of concentrated HNO_3 (2 ml) and concentrated HCl (6 ml) in a 1:3 ratio, known as aqua regia. The aqua regia solution is to be used within 15 to 20 min after its preparation, as it won't give desired results after a while. A USB microscope was used to inspect each sample and assess the depth and breadth of the weld.

3 Results & Discussion

Penetration depth is an important aspect of weld geometry. The two fundamental parameters used in the calculation of penetration depths in TIG welding are the weld current and the travel speed. Increasing the weld current resulted in an increase in the depth of penetration. At a given weld current, the depth of penetration decreases as travel speed increases. Attempts to increase the depth of penetration by raising the weld current lead to a wider weld profile with only marginal improvement in penetration.

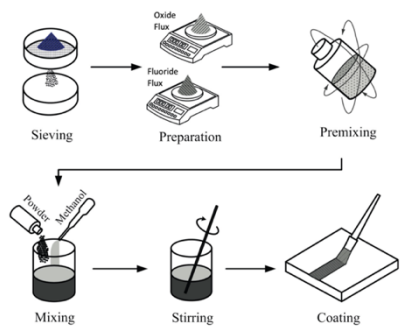


Fig 2.4. Preparation process for activated flux. [\[11\]](#)



Fig 2.5. Different Workpiece after Welding

3.1 Geometric Shape of Activated TIG Welds

Fig. 3.1. presents a transverse cross-section of stainless steel TIG welds produced without and with flux powder. Along with penetration depth, bead width and the depth-to-width ratio of all specimens.

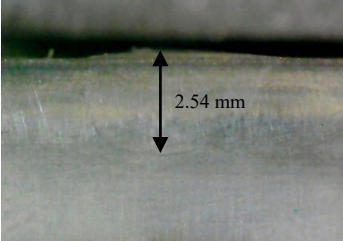
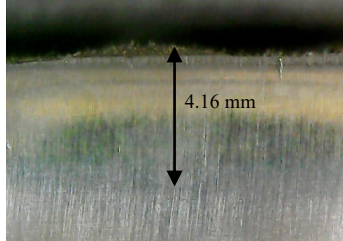
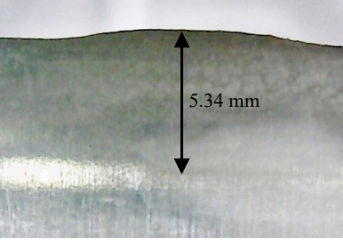
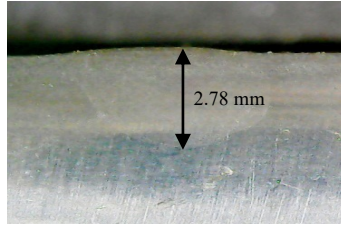
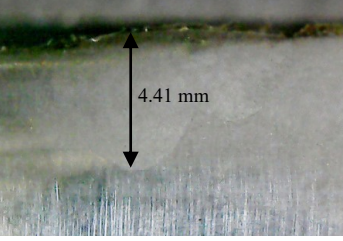
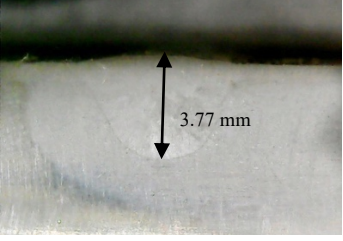
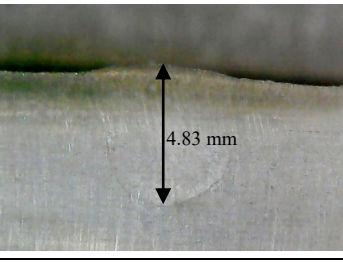
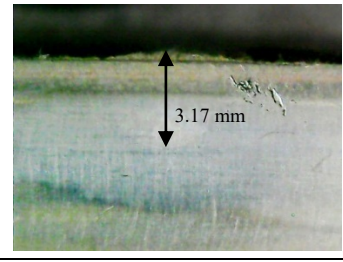
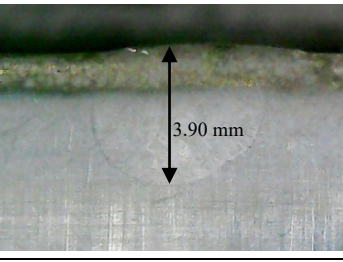
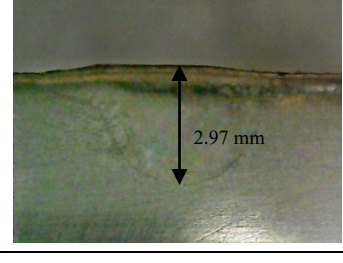
		
(a) Without Flux Powder (A1) Penetration depth: 2.54 mm Bead width: 6.83 mm Weld depth-to-width ratio: 0.37	(b) 50% Oxide Flux (Fe_2O_3) + 50% Fluoride Flux (NaF) (A2) Penetration depth: 4.16 mm Bead width: 6.92 mm Weld depth-to-width ratio: 0.60	(c) Only Oxide Flux (Fe_2O_3) (B1) Penetration depth: 5.34 mm Bead width: 6.51 mm Weld depth-to-width ratio: 0.82
		
(d) Only Fluoride Flux (NaF) (B2) Penetration depth: 2.78 mm Bead width: 8.94 mm Weld depth-to-width ratio: 0.31	(e) First Oxide Flux then Fluoride Flux (C1) Penetration depth: 4.41 mm Bead width: 9.13 mm Weld depth-to-width ratio: 0.48	(f) First Fluoride Flux then Oxide Flux (C2) Penetration depth: 3.77 mm Bead width: 6.74 mm Weld depth-to-width ratio: 0.55
		
(g) 80% Oxide Flux (Fe_2O_3) + 20% Fluoride Flux (NaF) (D1) Penetration depth: 4.83 mm Bead width: 5.89 mm Weld depth-to-width ratio: 0.82	(h) 20% Oxide Flux (Fe_2O_3) + 80% Fluoride Flux (NaF) (D2) Penetration depth: 3.17 mm Bead width: 8.05 mm Weld depth-to-width ratio: 0.39	(i) Oxide Flux on both sides of the welding region (E1) Penetration depth: 3.90 mm Bead width: 6.02 mm Weld depth-to-width ratio: 0.64
		
	(j) Fluoride Flux on both sides of the welding region (E2) Penetration depth: 2.97 mm Bead width: 8.02 mm Weld depth-to-width ratio: 0.37	

Fig 3.1. Effect of TIG Welding without and with various Flux Application

TIG welding without flux powder and with NaF powder generated a shallow, widespread profile, as shown in [Fig. 3.1, \(a\) and \(d\)](#) respectively. Fe₂O₃ powder created a deep, narrow profile, as seen in [Fig. 3.1\(c\)](#) giving the highest depth-to-width (aspect) ratio. Shown in [Fig. 3.1\(b\)](#), a mixture of equal quantities of both the flux powder is mixed, creating a less deep and broader weld as compared to [Fig. 3.1\(c\)](#). In [Fig. 3.1\(e\)](#), applying fluoride flux on oxide flux resulted in a deeper penetration than [Fig. 3.1\(d\)](#) but a broader weld bead, it is because of fluoride flux showing Centrifugal Marangoni Convection resulting in a broad weld bead. In [Fig. 3.1\(f\)](#), applying oxide flux on fluoride flux, developed a shallow and comparatively narrow weld bead, as oxide flux showing Centripetal Marangoni Convection resulting in a narrow weld bead. In [Fig. 3.1\(g\)](#), a mixture of oxide flux and fluoride flux in a 4:1 ratio results in a deep and narrow weld profile, similar to that of pure oxide flux. [Fig. 3.1\(h\)](#) shows a 4:1 blend of fluoride flux and oxide flux, giving a shallow and broad weld bead profile, similar to that of pure fluoride flux. In [Fig. 3.1\(i\) and \(j\)](#), oxide flux and fluoride flux is applied closely on both sides of the welding path respectively. In [Fig. 3.1\(i\)](#), the weld bead is deeper and narrow as compared to [Fig. 3.1\(a\)](#), because of Centripetal Marangoni Convection, the weld pool is pushed towards the centre of the weld and results in a narrow, deep weld bead profile. In [Fig. 3.1\(j\)](#), the weld bead is slightly deeper but very broad as compared to [Fig. 3.1\(a\)](#), the weld pool is pushed out from the weld centre due to Centrifugal Marangoni Convection, resulting in a larger and narrower weld bead shape.

The use of Fe₂O₃ powder in this study enabled maximum penetration in TIG welds of austenitic SS304 stainless steel. As a result, the addition of Fe₂O₃ powder can enhance the depth-to-width (aspect) ratio of TIG welds. A high aspect ratio in a weld indicates that the heat source has a high energy density, resulting in a concentrated heat input during the welding process. The overall heat needed per unit length of the weld reduces as the energy density of the heat source rises. As a result, active TIG welding is regarded as a greater energy density method. The ability of the heat source to melt the base metal is a crucial aspect of TIG welding. By A-TIG welding process, the deposition rate of welds can be increased without changing the weld current or travel speed. This implies that activated TIG welding has a superior melting efficiency. The application of activated flux in conventional TIG welding decreases the amount of arc heat necessary for welds that have a significant cross-sectional area and require deep joint penetration.

3.2 Surface Appearance of Activated TIG Welds

The surface appearances of TIG welds in stainless steel produced both with and without flux powder, are depicted in [Fig 3.2](#).

[Fig. 3.2\(a\)](#), shows the results of TIG welding without flux powder, which produces a smooth, coloured surface. [Fig. 3.2\(b\)](#), using a mixture of oxide and fluoride flux in equal amounts, results in no residual slag but spatter was produced in a small amount. [Fig. 3.2\(c\)](#), indicates that Fe₂O₃ powder produced little residual slag and a significant amount of spatter. [Fig. 3.2\(d\)](#), shows that no residual slag and spatter were produced using NaF powder. [Fig. 3.2\(e\) and \(f\)](#), shows that an uneven weld is produced, generating a large amount of spatter and no residual slag. [Fig. 3.2\(g\)](#), oxide flux being the major component and fluoride being the minor component of the flux mixture, resulted in a surface with a lot of spatter and little residual slag. [Fig. 3.2\(h\)](#), fluoride flux being the major component and oxide being the minor component of the flux mixture, resulted in a surface with a very less amount of spatter and no residual slag. [Fig. 3.2\(i\)](#), shows that little residual slag and a considerable amount of spatter were formed by Fe₂O₃ powder even on either side of the welding path. [Fig. 3.2\(j\)](#), shows that NaF powder on either side of the welding path did not result in any residual slag or splatter.

The results indicate that, in the case of stainless steel, TIG welds generated with NaF powder exhibit an appealing surface appearance, while Fe₂O₃ powder causes the development of slag and spatters. The low melting point, boiling point, and thermal decomposition temperature of fluoride compounds make them easily melted by the arc heat source used in TIG welding, which can account for the superior appearance of TIG welds created with NaF powder.

(a) Without Flux Powder (A1)	(b) 50% Oxide Flux (Fe_2O_3) + 50% Fluoride Flux (NaF) (A2)
(c) Only Oxide Flux (Fe_2O_3) (B1)	(d) Only Fluoride Flux (NaF) (B2)
(e) First Oxide Flux then Fluoride Flux (C1)	(f) First Fluoride Flux then Oxide Flux (C2)
(g) 80% Oxide Flux (Fe_2O_3) + 20% Fluoride Flux (NaF) (D1)	(h) 20% Oxide Flux (Fe_2O_3) + 80% Fluoride Flux (NaF) (D2)
(i) Oxide Flux on both sides of the welding region (E1)	(j) Fluoride Flux on both sides of the welding region (E2)

Fig 3.2 Influence of TIG Welding with different Flux Powder on Surface Appearance

4 Conclusion

- This study explored the effects of flux powders, NaF and Fe₂O₃, on the geometric shape of weld bead profiles through experimental investigation.
- The Fe₂O₃ welds generated slag and spatter, but the TIG welds made with NaF powder had an excellent surface appearance.
- The joint penetration and weld aspect ratio are both increased when TIG welding uses Fe₂O₃ powder.
- When Fe₂O₃ powder is used in TIG welding, Centripetal Marangoni Convection causes an increase in penetration depth while decreasing bead width. In contrast, the use of NaF powder in TIG welding does not significantly increase the weld aspect ratio because of Centrifugal Marangoni Convection.
- For the 17Cr-10Ni-2Mo alloys, the utilization of Fe₂O₃ powder in TIG welding can result in satisfactory performance and deep penetration.

5 References

- [1] Kuang-Hung Tseng, Development and application of oxide-based flux powder for tungsten inert gas welding of austenitic stainless steels, Powder Technology 233 (2013) 72–79
- [2] P.J. Modenesi, E.R. Apolinario, I.M. Pereira, TIG welding with single-component fluxes, Journal of Materials Processing Technology 99 (2000) 260–265.
- [3] H.Y. Huang, S.W. Shyu, K.H. Tseng, C.P. Chou, Evaluation of TIG flux welding on the characteristics of stainless steel, Science and Technology of Welding and Joining 10 (5) (2005) 566–573
- [4] S.W. Shyu, H.Y. Huang, K.H. Tseng, C.P. Chou, Study of the performance of stainless steel A-TIG welds, Journal of Materials Engineering and Performance 17 (2) (2008) 197–201.
- [5] T.S. Chern, K.H. Tseng, H.L. Tsai, Study of the characteristics of duplex stainless steel activated tungsten inert gas welds, Materials and Design 32 (1) (2011) 255–263.
- [6] K.H. Tseng, C.Y. Hsu, Performance of activated TIG process in austenitic stainless steel welds, Journal of Materials Processing Technology 211 (2011) 503–512.
- [7] C.R. Heiple, J.R. Roper, Effect of selenium on GTAW fusion zone geometry, Welding Journal 60 (8) (1981) 143–145
- [8] C.R. Heiple, P. Burgardt, Effects of SO₂ shielding gas additions on GTA weld shape, Welding Journal 64 (6) (1985) 159–162.
- [9] Kuang-Hung Tseng, Ko-Jui Chuang, Application of iron-based powders in tungsten inert gas welding for 17Cr–10Ni–2Mo alloys, Powder Technology 228 (2012) 36–46
- [10] C.R. Heiple, P. Burgardt, Effects of SO₂ shielding gas additions on GTA weld shape, Welding Journal 64 (6) (1985) 159–162
- [11] Pandya, D., Badgjar, A., & Ghetiya, N. (2021). A novel perception toward welding of stainless steel by activated TIG welding: A review. Materials Today: Proceedings, 45(2), 1662-1667. doi: 10.1016/j.matpr.2021.03.292
- [12] Kuang-Hung Tseng, Nai-Shien Wang, GTA welding assisted by mixed ionic compounds of stainless steel, Powder Technology 251 (2014) 52–60
- [13] Nayee, S. G., & Badheka, V. J. (2014). Effect of oxide-based fluxes on mechanical and metallurgical properties of Dissimilar Activating Flux Assisted-Tungsten Inert Gas Welds. Journal of Manufacturing Processes, 16(1), 80-88. doi: 10.1016/j.jmapro.2013.07.006